ASIAN JOURNAL OF CIVIL ENGINEERING (BUILDING AND HOUSING) VOL. 11, NO. 6 (2010)
PAGES 763-775

OPTIMIZING SINGLE-SPAN STEEL TRUSS BRIDGES WITH SIMULATED ANNEALING

O. Hasançebi[*a] and E. Doğan[b]
[a]Department of Civil Engineering, Middle East Technical University, Ankara, Turkey
[b]Department of Engineering Sciences, Middle East Technical University, Ankara, Turkey

ABSTRACT

This study presents applications of a simulated annealing integrated solution algorithm to the optimum design of single-span steel truss bridges subjected to gravity loadings. In the optimum design process of a bridge the members are sized simultaneously as the coordinates of the upper chord nodes are determined such that the least design weight is attained for the structure. The design constraints and limitations are imposed in accordance with serviceability and strength provisions of ASD-AISC (Allowable Stress Design Code of American Institute of Steel Institution) specification. A numerical example is presented, where optimum designs produced according to nine alternative topological forms of single-span truss bridges, namely Pratt, Parker, Baltimore, Pettit, K-Truss, Warren, Subdivided Warren, Quadrangular Warren and Whipple are compared for a selected span length of 600 ft (182.88 m) to quantify the influence of choice of a topological form on the final design weight of the bridge.

Keywords: Structural optimization; simulated annealing; single-span steel truss bridges; bridge topological forms; minimum weight design

1. INTRODUCTION

Over the years steel truss bridges have kept their popularity amongst bridge engineers. Apart from architectural attractiveness, these systems exhibit certain advantages from structural and constructional standpoints, such as speed of construction, durability, modification and repair, recycling, versatility, etc. They are rigid skeletal structures with straight members configured generally in some form of triangles to transfer the design loads from deck to the piers through mainly axial forces of the members. Single span steel truss bridges refer to a particular subset of these systems where the whole opening is crossed with a single span with generally simply supported end conditions. Especially, they are more preferable with respect to multi-span bridges in cases where disturbance to the stream bed needs to be avoided.

The single span truss bridges can be designed in a variety of different topological forms, such as Pratt, Parker, Baltimore, Pettit, K-Truss, Warren, Subdivided Warren, Quadrangular

[*] E-mail address of the corresponding author: oguzhan@metu.edu.tr (O. Hasançebi)

Warren, Whipple, etc. The Pratt truss has a topological feature such that the diagonals are all sloped in the same direction on each side of the truss around the mid-span. In this form of truss bridge, the upper chord and vertical members are subjected to compression whereas the diagonals and lower chord members are under tension. The Baltimore truss has additional bracing members in the lower section to prevent buckling in the compression members as well as to control deflection. Both Pratt and Baltimore trusses have a constant height throughout the span length of the bridge. The Parker and Pettit trusses have identical topological forms with Pratt and Baltimore trusses, respectively, except that the formers have a polygonal shape with the bridge height increasing from the ends towards the mid-span. In the Warren truss alternate diagonals sloped in different directions frame into each others at lower chord nodes. The Subdivided Warren truss has the topological form of Warren truss with vertical members having sub-diagonals and sub-verticals. The Quadrangular Warren is a double intersection truss form with alternating tension and compression diagonals. The K-truss is configured in the form of letter "K" by the orientation of the vertical member and two oblique members in each panel. Finally, the Whipple truss is the one having elongated and usually thin tension members which cross two or more members.

In the present study, optimum design of single-span steel truss bridges is investigated in conjunction with simulated annealing (SA) optimization technique. The SA employs a meta-heuristic numerical optimization procedure, the theory of which extends to the annealing process of physical systems in thermodynamics [1]. In this process a physical system (a solid or a liquid) initially at a high-energy state is cooled down to reach the lowest energy state. The idea that this process can be simulated to solve optimization problems was put forward by Kirkpatrick et al. [2] by establishing a direct analogy between minimizing the energy level of a physical system and lowering the cost of an objective function. The successful applications of the technique in the fields of structural optimization and computational structural mechanics have been reported in a number of publications in the literature, such as Refs. [3-8].

In the solution process both size and shape variables are employed simultaneously by the SA algorithm to minimize the design weight of a bridge. Size variables are used to determine the required steel sections for the bridge members to satisfy strength and serviceability requirements imposed according to provisions of ASD-AISC [9] standard. Shape variables, on the other hand, are utilized to find the best height or shape of the upper chord of a bridge. The application of the solution algorithm developed is illustrated with a numerical design example, where the optimum designs produced according to abovementioned nine different topological forms of single-span bridges are compared for a selected span length of 600 ft (182.88 m). This way, the weight efficiency of various topological forms is investigated and it is shown that the choice of a topological form has a great impact on the final design weight of the bridge.

2. OPTIMUM DESIGN PROBLEM FORMULATION

In the optimum design process of a single-span steel truss bridge, it is required to select the structural members from a standard steel section table as well as to determine the height or shape of the upper chord of the bridge such that the structure satisfies the strength and serviceability limitations imposed by a code of practice, while the minimum weight of the bridge is attained. The formulation of design constraints according to ASD–AISC [9] yields the following mixed discrete programming problem.

Find a vector of size design variables ***A*** and a vector of shape design variables ***S***,

$$\mathbf{A}^T = \left[A_1, A_2, ..., A_{N_m}\right] \text{ and } \boldsymbol{S}^T = \left[S_1, S_2, ..., S_{N_s}\right] \tag{1}$$

to minimize the weight of the bridge (*W*),

$$W = \sum_{m=1}^{N_m} \rho_m L_m A_m \tag{2}$$

subject to a set of behavioural and performance limitations expressed as

$$g_m = \frac{\sigma_m}{(\sigma_m)_{all}} - 1 \leq 0, \quad m = 1,.., N_m \tag{3}$$

$$s_m = \frac{\lambda_m}{(\lambda_m)_{all}} - 1 \leq 0, \quad m = 1,.., N_m \tag{4}$$

$$\delta_{j,k} = \frac{d_{j,k}}{(d_{j,k})_{all}} - 1 \leq 0, \quad j = 1,.., N_j \tag{5}$$

In Eqns. (1)-(5), N_m is the total number of bridge members; $A_m\ L_m, \rho_m$ are the cross-sectional area, length and unit weight of the *m*-th bridge member, respectively; S_j is the *j*-th shape variable; N_s is the total number of shape variables associated with the coordinates of the upper chord nodes of the bridge; the functions g_m, s_m and $\delta_{j,k}$ are referred to as constraints being bounds on stresses, slenderness ratios and displacements, respectively; σ_m and $(\sigma_m)_{all}$ are the computed and allowable axial stresses for the *m*-th member, respectively; λ_m and $(\lambda_m)_{all}$ are the slenderness ratio and its upper limit for *m*-th member, respectively; N_j is the total number of nodes in the bridge; and finally $d_{j,k}$ and $(d_{j,k})_{all}$ are the displacements computed in the *k*-th direction of the *j*-th node and its permissible value, respectively.

According to ASD-AISC [9], the maximum slenderness ratio is limited to 300 and 200 for tension and compression members, respectively. Therefore, the slenderness related design constraints can be formulated as follows:

$$\lambda_m = \frac{K_m L_m}{r_m} \leq \begin{matrix} 300 & \text{(for tension members)} \\ 200 & \text{(for compression members)} \end{matrix} \qquad (6)$$

where K_m is the effective length factor of m-th member ($K_m = 1$ for all members), and r_m is its minimum radii of gyration.

The allowable tensile stresses for tension members are calculated as in Eqn. (7).

$$(\sigma_t)_{all} = 0.60F_y \text{ and } (\sigma_t)_{all} = 0.50F_u \qquad (7)$$

where F_y and F_u stand for the yield and ultimate tensile strengths, and the smaller of the two formulas is considered to be the upper level of axial stress for a tension member.

The allowable stress limits for compression members are calculated depending on two possible failure modes of the members known as elastic and inelastic buckling, Eqn. (8)

$$(\sigma_c)_{all} = \begin{cases} \dfrac{\left[1 - \dfrac{(K_m L_m / r_m)^2}{2C_c^2}\right] F_y}{\dfrac{5}{3} + \dfrac{3(K_m L_m / r_m)}{8C_c} - \dfrac{(K_m L_m / r_m)^3}{8C_c^3}} & , \ \lambda_m < C_c \text{ (inelastic buckling)} \\ \dfrac{12\pi^2 E}{23(K_m L_m / r_m)^2} & , \ \lambda_\mathrm{m} \geq C_c \text{ (elastic buckling)} \end{cases} \qquad (8)$$

where E is the modulus of elasticity, and $C_c = \sqrt{2\pi^2 E / F_y}$ is the critical slenderness ratio between elastic and inelastic buckling.

3. SIMULATED ANNEALING ALGORITHM

The basic computational steps of simulated annealing algorithm are outlined in the following. The further enhancement of the algorithm that results in additional performance of the technique can be found in Hasançebi et al. [10].

Step 1. Cooling schedule: The first step is the setting of an appropriate cooling schedule. After choosing suitable values for the starting acceptance probability (P_s), the final acceptance probability (P_f), and the number of cooling cycles (N_c), the cooling schedule parameters are calculated as follows:

$$T_s = -\frac{1}{\ln(P_s)}, \quad T_f = -\frac{1}{\ln(P_f)}, \quad \eta = \left[\frac{\ln(P_s)}{\ln(P_f)}\right]^{1/N_c - 1} \qquad (9)$$

In Eqn. (9), T_s, T_f and η are referred to as starting temperature, final temperature, and cooling factor, respectively. The starting temperature is assigned as the current temperature of the process, i.e., $T = T_s$.

Step 2. Initial Design: Next, an initial design is originated via random initialization in a way such that size variables are set to arbitrary ready sections selected from a standard profile list and shape variables are assigned to any values between their lower and upper bounds. The analysis of the bridge is then performed and the force and deformation responses are obtained under the applied loads. If all the constraints are satisfied, the objective function value (ϕ) of the design is directly computed from Eqn. (2), i.e., $\phi = W$. If, however, the design violates some of the problem constraints, it is penalized and its objective function value is calculated from Eqn. (10).

$$\phi = W\left[1 + \alpha\left(\sum_i c_i\right)\right] \tag{10}$$

In Eqn. (10), c_i is the *i*-th problem constraint of the problem at hand, and α is the penalty coefficient used to tune the intensity of penalization as a whole. It is set to an appropriate static value, such as $\alpha = 1$.

Step 3. Generating candidate designs: A number of candidate designs are generated in the close vicinity of the current design. This is carried out as follows: (i) either a size or shape design variable is selected, (ii) the selected variable is given a small perturbation in a predefined neighborhood, and (iii) finally, a candidate design is generated by assuming the perturbed value of the variable, while keeping all others same as in the current design. It follows that a candidate design differs from the current one in terms of one design variable only. It is important to note that each design variable is selected only once in a random order to originate a candidate design. Hence, the total number of candidate designs generated in a single iteration of the cooling cycle is equal to the number of design variables.

Step 4. Evaluation of a candidate design: Each time when a candidate design is generated, its objective function value (ϕ) is computed first and then it is set to compete with the current design. If the candidate provides a better solution, it is accepted automatically and it replaces the current design. Otherwise, the so-called Metropolis test is employed to determine the winner, in which case the probability of accepting a poor candidate (P) is assigned as follows:

$$P = \exp(-\Delta\phi / KT)\text{, where } \Delta\phi = \phi_a - \phi_c \geq 0 \tag{11}$$

In Eqn. (11), ϕ_c and ϕ_a are the objective function values of the current and candidate designs, respectively; T is the current temperature of the process; and K is the Boltzman parameter which is manipulated as the working average of positive $\Delta\phi$ values.

Step 5. Iterations of a Cooling Cycle: A single iteration of a cooling cycle is referred to the case where all design variables are selected once and perturbed to generate candidate designs. Generally, a cooling cycle is iterated a certain number of times in the same manner to ensure that the objective function is reduced to a reasonably low value associated with the temperature of the cooling cycle. Having selected the iterations of the starting and final cooling cycles (i_s and i_f), the iteration of a cooling cycle (i_c) at a given temperature T is determined by a linear interpolation between i_s and i_f, as follows:

$$i_c = i_f + (i_f - i_s)\left(\frac{T - T_f}{T_f - T_s}\right) \tag{12}$$

Step 6. Reducing Temperature: After the cooling cycle is iterated a number of times, the temperature is reduced by the ratio of the cooling factor η, and the temperature of the next cooling cycle is set as in Eqn. (13)

$$T^{k+1} = T^k \eta \tag{13}$$

where T^k and T^{k+1} denote the temperature at the k and (k+1)-th cooling cycles, respectively.

4. NUMERICAL EXAMPLE

A numerical design example is studied here, (i) to verify and demonstrate the applicability of the solution algorithm to the optimum design of single-span steel truss bridges, (ii) to explore the weight efficiency of various topological forms of a bridge under gravity loads, and finally (iii) to emphasize the significance of a bridge topological form on its final design weight.

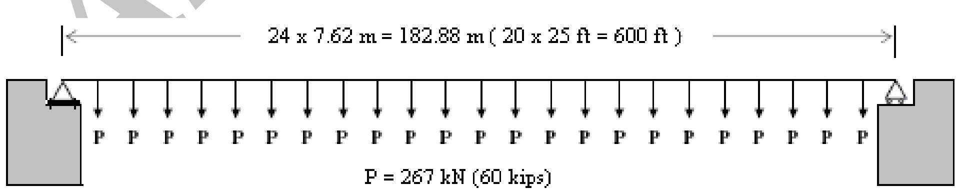

Figure 1. A single-span steel truss bridge design example

In the example it is intended to build up a single-span steel truss bridge to cross an opening of 600 ft (182.88 m). Only the lower chord of the bridge is geometrically defined as shown in Figure 1, and it consists of 25 panel points equally spaced at 25 ft (7.62 m). The design loads are calculated according to the provisions of ASCE 7-05 [11]. Live loads resulted from traffic are combined with dead loads of the deck and floor systems, which are later on transmitted to the lower chord, resulting in equivalent panel point loads of 60 kips (267 kN) each in each model.

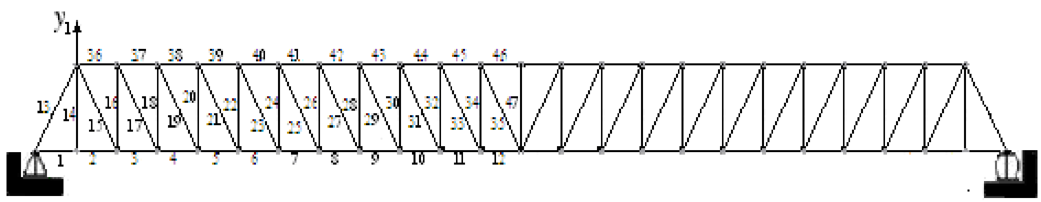

a) Pratt truss

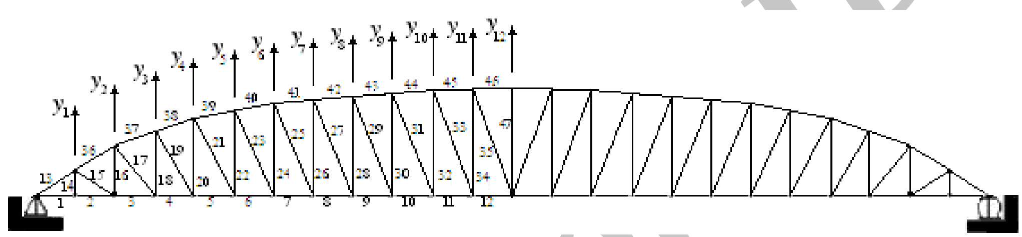

b) Parker truss

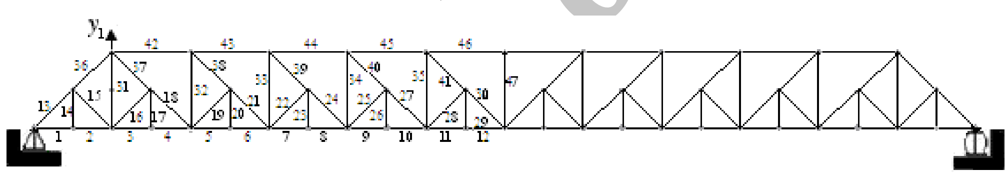

c) Baltimore truss

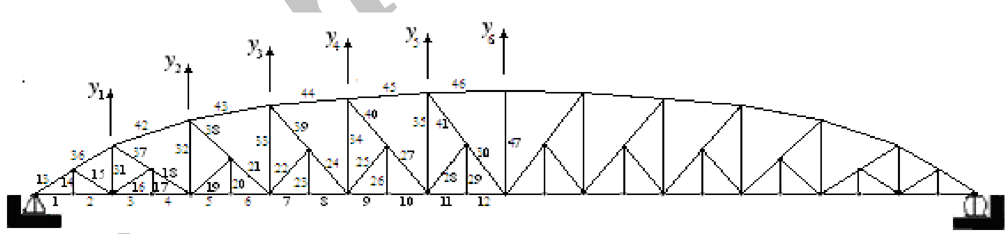

d) Pettit truss

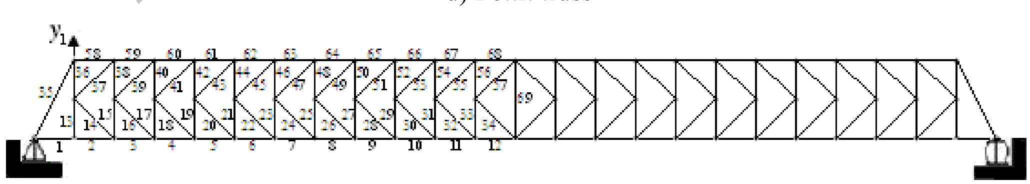

e) K-truss

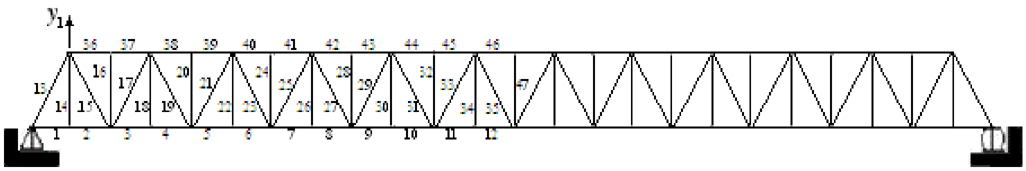

f) Warren truss

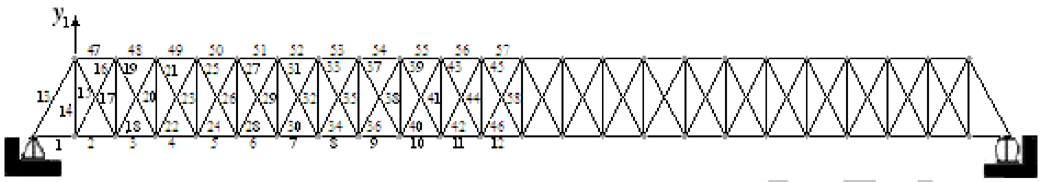

g) Quadrangular Warren truss

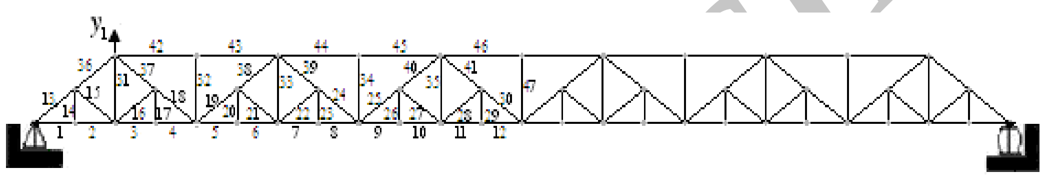

h) Subdivided Warren Truss

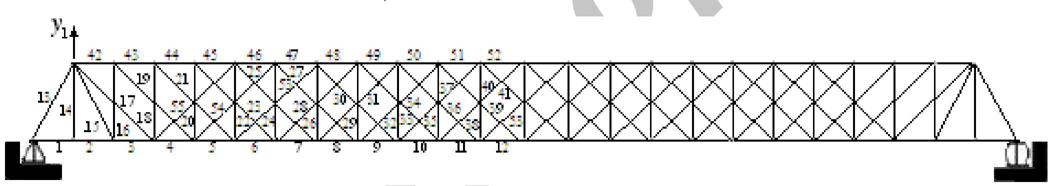

i) Whipple truss

Figure 2. Bridge topological forms: a) Pratt, b) Baltimore, c) Pettit, d) Baltimore, e) K-truss, f) Warren, g) Quadrangular Warren, h) Subdivided Warren, i) Whipple

To comprise the superstructure, nine alternative topological forms of single-span truss bridges shown in Figure 2 are considered. In the optimum design process with each topological form, both size and shape design variables are employed together. Size variables are used to determine the required steel sections for bridge members and are grouped considering the symmetry of the structures around mid-span. Hence, the number of independent size variables used in a model is equal to half of the total number of members in the model. The size variables are selected from a total of 83 wide-flange ready sections ranging between W10x12 and W14x730. The shape variables are chosen to define the height or shape of the upper chord of a bridge model, again considering a desired symmetry of the structure about mid-span. The number of shape variables used in a model depends on the bridge topological form. For instance, a single shape variable is used to define the height of the truss in Pratt, Baltimore, Warren, Subdivided Warren, Quadrangular Warren, Whipple and K-truss forms, since these forms have straight upper chords. In Parker and Pettit forms, however, the y-coordinates of all upper chord nodes are allowed to vary, resulting in 12 and

6 independent shape variables, respectively. The ranges of shape variables are chosen between zero and half of the span length ($L/2$ =150 ft = 91.44 m). In all the bridge models, the strength and stability requirements of the designs are specified as per ASD-AISC [9] provisions, plus the maximum displacements of panel points in any direction are restricted to 1/600 of the total span length. The following material properties of the steel are used in all the models: F_y (yield stress) = 36 ksi (2531 kg/cm^2) and E (modulus of elasticity) = 29,000 ksi (2,038,936 kg/cm^2).

The optimum design of the bridge under each of the nine topological forms was sought by running the solution algorithm five times independently due to stochastic nature of the SA technique. The control parameters are set to the following values in these runs in line with recommendations of the former studies [10, 12-14]: $P_s = 0.50$, $P_f = 10^{-3}$, $i_s = 1$, $i_f = 5$, $N_c = 300$, resulting in the cooling schedule parameters T_s= 1.4427, T_f = 0.1448 and η = 0.9923 from Eqn. (10). The average computing time for a single run takes about 12 min on a serial computer with Intel Quad Core Q9300 2.5GHZ LGA775 processor.

The best (optimum) designs obtained for the bridge under nine different topological forms are tabulated in Table 1 with section designations attained for each member group and the resulting values of shape variables in conjunction with design variable numbering shown in Figure 2 for each model. The minimum weight design for the bridge is produced by Pettit truss with a design weight of 624,277.4 lb (283,172.2 kg). This design is followed by Parker truss with the corresponding design weight of 722,558.3 lb (327,752. 4 kg). It is interesting to note that both of these truss forms have a varying bridge height. Although a polygonal shape is not enforced by any sort of constraints, the resulting shapes of the bridges generated in the optimum design process confirm with this particular shape naturally. As compared to Parker model, Pettit truss results in smaller member lengths, in which intermediate panel points are defined between upper and lower chords to keep the member lengths within reasonable limits, and thereby increasing the buckling strength of the members significantly. Nevertheless, both truss forms outperform all the others with straight upper chords (constant bridge height models). Amongst the trusses with straight upper chords, the subdivided forms (K-truss, Subdivided Warren and Baltimore) perform more efficiently with the corresponding design weights of 830,048.1 lb (376,509.8 kg), 855,874.5 lb (388,224.7 kg) and 869,646.4 lb (394,471.6 kg), respectively owing to the increased buckling strength of the members in these models. The largest design weights for the bridge are produced by Pratt and Whipple trusses with design weights of 1,379,721.2 lb (625,841.5 kg) and 1,384,147.8 lb (627,849.4 kg), respectively. The design history curve representing the variation of the best feasible obtained thus far in the optimum design process is plotted in Figure 3 for each model.

Table 1: Optimum designs obtained for the bridge under each topological form.

Variable	Bridge topological forms								
	Pratt	**Parker**	**Baltimore**	**Pettit**	**K_truss**	**Warren**	**Q_Warren**	**S_Warren**	**Whipple**
	Size variables, ready sections								
A_1	W12x136	W14x176	W12x152	W12x152	W10x68	W14x145	W14x74	W12x190	W14x109
A_2	W12x79	W12x279	W12x210	W14x193	W10x77	W12x79	W12x96	W12x170	W12x152
A_3	W12x279	W12x230	W14x120	W14x159	W12x136	W14x455	W14x211	W12x190	W12x305
A_4	W14x342	W14x398	W14x145	W14x159	W12x210	W12x252	W14x311	W14x132	W14x370
A_5	W14x426	W12x336	W14x257	W12x170	W12x252	W14x370	W14x370	W12x336	W14x730
A_6	W14x605	W14x426	W12x279	W12x170	W14x342	W14x665	W14x455	W12x305	W14x730
A_7	W14x550	W14x455	W14x342	W12x190	W14x398	W12x279	W14x426	W12x336	W14x665
A_8	W14x730	W14x605	W14x370	W12x190	W14x455	W14x605	W14x605	W14x257	W14x283
A_9	W14x730	W14x426	W14x500	W14x211	W14x455	W14x730	W14x500	W14x426	W14x730
A_{10}	W14x730	W14x500	W14x730	W12x190	W14x550	W14x730	W14x730	W14x550	W14x730
A_{11}	W14x730	W14x500	W14x730	W14x193	W14x550	W14x605	W14x730	W14x398	W14x730
A_{12}	W14x730	W14x605	W14x500	W12x190	W14x550	W14x730	W14x730	W14x730	W14x730
A_{13}	W14x550	W14x342	W14x311	W14x311	W12x26	W14x550	W14x550	W14x342	W14x455
A_{14}	W12x53	W14x74	W10x26	W14x43	W12x136	W12x79	W12x53	W14x34	W10x49
A_{15}	W14x257	W14x132	W10x49	W10x60	W14x99	W14x233	W14x211	W10x100	W14x176
A_{16}	W14x426	W12x79	W10x49	W10x88	W14x120	W14x132	W14x145	W12x170	W14x176
A_{17}	W12x336	W12x120	W12x26	W12x35	W14x90	W14x500	W14x90	W12x65	W12x152
A_{18}	W14x398	W12x87	W12x210	W12x65	W10x112	W14x74	W14x342	W14x193	W14x90
A_{19}	W14x311	W12x65	W10x49	W12x65	W14x90	W12x252	W12x87	W14x233	W12x210
A_{20}	W14x370	W12x40	W12x26	W10x39	W10x112	W14x90	W12x53	W14x30	W14x90
A_{21}	W14x257	W10x49	W12x170	W10x45	W12x79	W14x455	W10x112	W12x87	W12x65
A_{22}	W14x311	W10x49	W10x54	W14x90	W10x100	W12x65	W14x211	W12x65	W10x88
A_{23}	W12x252	W14x74	W12x26	W10x39	W12x72	W14x159	W10x49	W12x30	W12x65
A_{24}	W14x257	W14x90	W12x170	W12x58	W10x100	W14x233	W14x233	W14x176	W10x49
A_{25}	W14x211	W12x65	W10x49	W14x109	W12x65	W14x311	W12x96	W12x190	W12x65
A_{26}	W14x233	W10x60	W12x26	W10x68	W14x82	W10x88	W10x49	W10x26	W10x49
A_{27}	W12x190	W12x65	W12x120	W14x82	W10x54	W12x120	W12x96	W10x68	W12x210
A_{28}	W14x193	W12x72	W10x49	W14x99	W12x79	W14x90	W14x176	W14x109	W12x65
A_{29}	W14x211	W12x65	W10x39	W10x54	W10x49	W14x233	W10x49	W10x39	W14x99
A_{30}	W14x159	W12x65	W12x40	W10x60	W10x60	W10x68	W14x176	W14x48	W12x252
A_{31}	W12x210	W12x72	W12x65	W12x45	W10x49	W14x176	W12x72	W12x136	W12x65
A_{32}	W14x120	W12x72	W14x342	W10x49	W14x48	W14x120	W10x49	W12x136	W14x90
A_{33}	W12x120	W14x109	W14x283	W14x99	W12x26	W14x176	W12x72	W12x87	W12x65
A_{34}	W14x159	W12x65	W14x193	W14x90	W10x33	W12x65	W14x145	W14x211	W14x455
A_{35}	W12x96	W14x90	W14x176	W14x145	W14x665	W14x120	W12x53	W12x120	W10x49
A_{36}	W12x305	W14x342	W14x283	W14x283	W12x230	W14x283	W14x145	W14x283	W12x65
A_{37}	W14x283	W14x370	W12x210	W12x45	W14x159	W12x190	W12x65	W14x145	W14x455
A_{38}	W14x370	W14x550	W12x252	W10x77	W14x109	W14x398	W10x49	W12x279	W10x49
A_{39}	W14x730	W14x426	W14x145	W10x33	W14x109	W14x342	W12x65	W14x193	W14x109
A_{40}	W14x730	W14x426	W14x109	W12x58	W14x109	W14x730	W14x145	W14x193	W12x65
A_{41}	W14x730	W14x455	W10x88	W10x54	W14x145	W14x500	W10x49	W12x136	W12x65

Variable	Bridge topological forms								
	Pratt	**Parker**	**Baltimore**	**Pettit**	**K_truss**	**Warren**	**Q_Warren**	**S_Warren**	**Whipple**
A_{42}	W14x730	W14x455	W14x398	W14x550	W12x96	W14x730	W14x145	W14x426	W14x370
A_{43}	W14x730	W14x398	W14x550	W14x550	W14x132	W14x605	W12x72	W14x398	W14x550
A_{44}	W14x730	W14x550	W14x605	W14x500	W10x88	W14x730	W10x49	W14x730	W14x550
A_{45}	W14x730	W14x605	W14x665	W14x500	W14x109	W14x730	W12x65	W14x605	W14x500
A_{46}	W14x730	W14x550	W14x730	W14x500	W10x88	W14x730	W14x145	W14x730	W14x550
A_{47}	W10x49	W12x65	W12x65	W14x176	W14x99	W10x100	W14x145	W12x72	W14x730
A_{48}	N/A	N/A	N/A	N/A	W12x72	N/A	W12x210	N/A	W14x730
A_{49}	N/A	N/A	N/A	N/A	W14x99	N/A	W14x311	N/A	W14x730
A_{50}	N/A	N/A	N/A	N/A	W10x68	N/A	W14x426	N/A	W14x730
A_{51}	N/A	N/A	N/A	N/A	W12x87	N/A	W14x398	N/A	W14x730
A_{52}	N/A	N/A	N/A	N/A	W12x53	N/A	W14x665	N/A	W14x730
A_{53}	N/A	N/A	N/A	N/A	W12x65	N/A	W14x550	N/A	W14x455
A_{54}	N/A	N/A	N/A	N/A	W12x53	N/A	W14x730	N/A	W14x455
A_{55}	N/A	N/A	N/A	N/A	W12x65	N/A	W14x730	N/A	W14x455
A_{56}	N/A	N/A	N/A	N/A	W12x40	N/A	W14x730	N/A	N/A
A_{57}	N/A	N/A	N/A	N/A	W12x65	N/A	W14x730	N/A	N/A
A_{58}	N/A	N/A	N/A	N/A	W12x79	N/A	W12x53	N/A	N/A
A_{59}	N/A	N/A	N/A	N/A	W12x152	N/A	N/A	N/A	N/A
A_{60}	N/A	N/A	N/A	N/A	W14x211	N/A	N/A	N/A	N/A
A_{61}	N/A	N/A	N/A	N/A	W14x283	N/A	N/A	N/A	N/A
A_{62}	N/A	N/A	N/A	N/A	W14x342	N/A	N/A	N/A	N/A
A_{63}	N/A	N/A	N/A	N/A	W14x398	N/A	N/A	N/A	N/A
A_{64}	N/A	N/A	N/A	N/A	W14x455	N/A	N/A	N/A	N/A
A_{65}	N/A	N/A	N/A	N/A	W14x500	N/A	N/A	N/A	N/A
A_{66}	N/A	N/A	N/A	N/A	W14x550	N/A	N/A	N/A	N/A
A_{67}	N/A	N/A	N/A	N/A	W14x550	N/A	N/A	N/A	N/A
A_{68}	N/A	N/A	N/A	N/A	W14x665	N/A	N/A	N/A	N/A
A_{69}	N/A	N/A	N/A	N/A	W12x65	N/A	N/A	N/A	N/A
					Shape variables (in.)				
y_1	739	222	802	450	867	726	733	810	638
y_2	N/A	363	N/A	736	N/A	N/A	N/A	N/A	N/A
y_3	N/A	445	N/A	956	N/A	N/A	N/A	N/A	N/A
y_4	N/A	549	N/A	1110	N/A	N/A	N/A	N/A	N/A
y_5	N/A	640	N/A	1157	N/A	N/A	N/A	N/A	N/A
y_6	N/A	704	N/A	1167	N/A	N/A	N/A	N/A	N/A
y_7	N/A	769	N/A	N/A	N/A	N/A	N/A	N/A	N/A
y_8	N/A	817	N/A	N/A	N/A	N/A	N/A	N/A	N/A
y_9	N/A	860	N/A	N/A	N/A	N/A	N/A	N/A	N/A
y_{10}	N/A	887	N/A	N/A	N/A	N/A	N/A	N/A	N/A
y_{11}	N/A	895	N/A	N/A	N/A	N/A	N/A	N/A	N/A
y_{12}	N/A	900	N/A	N/A	N/A	N/A	N/A	N/A	N/A
Weight,lb (kg)	1379721.2 (625841.5)	722558.3 (327752.4)	869646.4 (394471.6)	624277.4 (283172.2)	830048.1 (376509.8)	1150368.2 (521807.0)	1090091.5 (494465.5)	855874.5 (388224.7)	1384147.8 (627849.4)

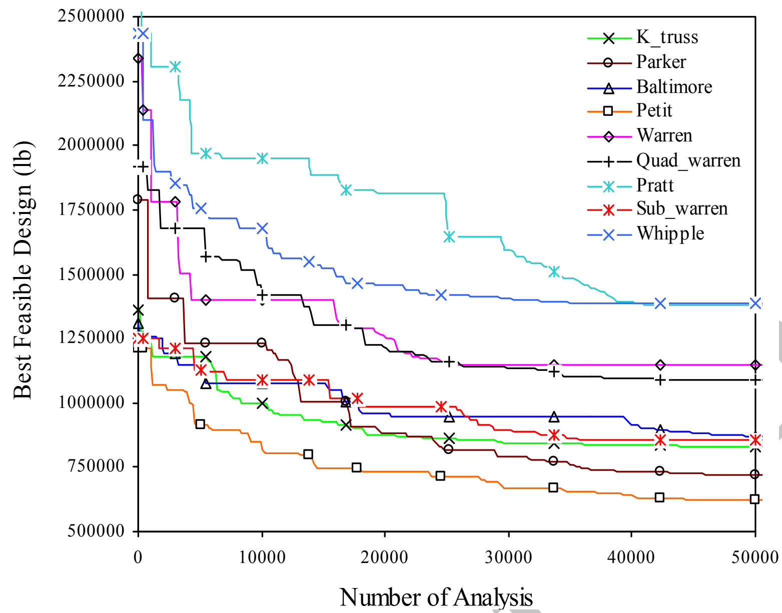

Figure 3. The design history curve of the best solution for each topological form.

5. CONCLUSIONS

This study concerns with application of a SA integrated solution algorithm to the optimum design of single-span steel truss bridges. In the study, a bridge with a certain span length is first configured according to nine topological forms commonly used for single-span steel truss bridges, and the resulting structures are sized and shaped simultaneously for the minimum design weight subject to strength, stability and displacement provisions of ASD-AISC [9]. The optimum design produced for the bridge is 624,277.4 lb (283,172.4 kg) with the most favourable model (Pettit) and 1,384,147.8 lb (627,849.4 kg) with the most unfavourable model (Whipple), indicating that an appropriate choice of the bridge topological model may lead to savings in material as much as 62 %. However, it should be kept in mind that the cost of construction of the bridge cannot directly be related to its weight; rather it is influenced by many other factors, including the type and number of joints used in the structure, etc. For the design example considered here, Pettit and Parker trusses, which have polygonal upper chords, turn out to be the most weight-effective models, outperforming all the other forms with straight upper chords. Additional studies are required to investigate the cost-efficiency of the bridge models with respect to a set of parameters, such as span length, design loads, constraints, etc.

REFERENCES

1. Metropolis N, Rosenbluth AW, Rosenbluth M, Teller A, Teller H. Equations of state

calculations by fast computing machines, J. Chem. Phys. **21**(1953) 1087–91.
2. Kirkpatrick S, Gelatt CD, Vecchi MP. Optimization by simulated annealing, Science, **220**(1983) 671–80.
3. Balling RJ. Optimal steel frame design by simulated annealing, *Journal of Structural Engineering*, No. 6, **117**(1991) 1780–95.
4. Chen GS, Bruno RJ, Salama M. Optimal placement of active/passive members in truss structures using simulated annealing, AIAA Journal, No. 8. **29**(1991) 815–27.
5. Shim PY, Manoochehri S. Generating optimal configurations in structural design using simulated annealing, *International Journal for Numerical Methods in Engineering*, **40**(1997) 1053–69.
6. Ceramic B, Fryer C, Baires RW. An application of simulated annealing to the optimum design of reinforced concrete retaining structures, *Computers and Structures*, **79**(2001) 1569–81.
7. Erdal O, Sönmez FO. Optimum design of composite laminates for maximum buckling load capacity using simulated annealing, *Composite Structures*, 71(2005) 45–52.
8. Değertekin SÖ. A comparison of simulated annealing and genetic algorithm for optimum design of nonlinear steel space frames, Structural and Multidisciplinary Optimization, **34**(2007) 347–59.
9. *Manual of Steel Construction, Allowable Stress Design*, 9th edition, AISC, American Institutes of Steel Construction, Inc, Chicago, Illinois, USA, 1989.
10. Hasançebi O, Çarbaş S, Saka MP. Improving the performance of simulated annealing in structural optimization, *Journal of Structural and Multidisciplinary Optimization*, **41**(2010) 189–203.
11. ASCE 7-05, Minimum Design Loads for Building and Other Structures, 2005.
12. Bennage WA, Dhingra AK. Single and multi-objective structural optimization in discrete-continuous variables using simulated annealing, *International Journal in Numerical Methods in Engineering*, **38**(1995) 2753–73.
13. Hasançebi O, Erbatur F. On efficient use of simulated annealing in complex structural optimization problems, *Acta Mech*, **157**(2002) 27–50.
14. Hasançebi O, Erbatur F. Layout optimisation of trusses using simulated annealing, *Adv Eng Softw*, **33**(2002) 681–96.